Journal of Alloys and Compounds 514 (2012) 120–126

Contents lists available at SciVerse ScienceDirect

Journal of Alloys and Compounds

journal homepage: www.elsevier.com/locate/jallcom

Magnetic properties of a $DyFe_5Al_7$ single crystal

D.I. Gorbunov [a,b,*], A.V. Andreev [a], N.V. Mushnikov [b]

[a] *Institute of Physics, Academy of Sciences, Na Slovance 2, 182 21 Prague, Czech Republic*
[b] *Institute of Metal Physics, Ural Branch of Russian Academy of Sciences, Kovalevskaya 18, 620990 Ekaterinburg, Russia*

ARTICLE INFO

Article history:
Received 5 September 2011
Received in revised form 3 November 2011
Accepted 3 November 2011
Available online 22 November 2011

Keywords:
Rare-earth intermetallics
Magnetic anisotropy
Ferrimagnetism
Field-induced transition

ABSTRACT

A single crystal of $DyFe_5Al_7$ (tetragonal $ThMn_{12}$ structure) has been studied. $DyFe_5Al_7$ orders ferrimagnetically at $T_C = 231$ K and has a compensation of the Dy and Fe sublattices at $T_{comp} = 93$ K. Magnetization isotherms measured along the principal axes of the single crystal indicate that the magnetic moments lie in the basal plane of the tetragonal lattice. Strong magnetic anisotropy is observed not only between the basal plane and the [0 0 1] axis but also within the basal plane, with the [1 0 0] axis being the easy magnetization direction with the spontaneous magnetic moment $2.1\mu_B$. A very high coercivity with H_c values up to 3 T was found at 2 K. In the temperature range 75–100 K, the compound exhibits a field-induced magnetic transition along the easy [1 0 0] direction. Temperature dependence of the critical field H_{cr} of the transition is very strong, the value of H_{cr} evidently exceeds 14 T below 75 K. A model for the magnetization process of a two-sublattice ferrimagnet with a weak intersublattice exchange interaction has been developed to explain the magnetic transition. The model reproduces the temperature behavior of H_{cr} near the compensation point.

1. Introduction

Intermetallic compounds based on rare-earth R and 3d-transition elements attract a lot of attention due to their intrinsic magnetic properties determined by localized magnetism of the rare-earth sublattice and itinerant electron magnetism of the 3d-metal sublattice. A great variety of such compounds have already been studied, yet some phenomena observed remain to be understood. In this respect one of the most interesting objects are compounds with the formula RFe_5Al_7 (R–Y, Sm–Lu) due to their unusual magnetic properties: negative magnetization (antiparallel to the field direction), strong thermal and magnetic hysteresis, time-dependent effects [1].

The RFe_5Al_7 compounds crystallize in the tetragonal $ThMn_{12}$-type structure (space group *I*4/*mmm*) with two formula units per elementary cell. The R atoms occupy the 2a sites, whereas the Fe and Al atoms are distributed over the 8f, 8j and 8i sites. It was found that the Fe atoms readily fill the 8f sites and then the 8j sites [2–6]. The Al atoms occupy mainly the 8i sites and share the 8j sites with the Fe atoms.

Magnetic properties of the RFe_5Al_7 compounds have been thoroughly studied on polycrystalline samples. The compounds with heavy R elements order ferrimagnetically with the Curie temperatures T_C varying from 207 to 268 K [2–4,7]. It was found that the intra-sublattice 2a–2a and 8j–8j exchange interactions are ferromagnetic, whereas the inter-sublattice 2a–8j interactions are antiferromagnetic (AF). Controversy exists whether the Fe magnetic moments in the 8f sites are ordered antiferromagnetically [2,3] or ferromagnetically [4].

The negative magnetization, thermal and magnetic hysteretic phenomena, time-dependent effects are all related to a strong anisotropy of the RFe_5Al_7 compounds as suggested in [2]. Although their magnetic anisotropy has never been investigated in detail, neutron diffraction experiments made it possible to determine that the magnetic moments of the compounds with R = Tb, Dy, Er and Tm lie in the basal plane, while those of the compound with R = Ho are aligned along the *c* axis of the tetragonal lattice [4]. Coercivity of almost all compounds with magnetic rare-earth elements noticeably exceeds 1 T at 4.1 K. In ref. [2] it is assumed to indicate strong magnetic anisotropy. However, this conclusion should be verified by a direct measurement of the anisotropy field since the relation between the coercivity and anisotropy is rather complicated.

In order to obtain detailed information on the magnetic properties of the RFe_5Al_7 compounds, their single crystals are highly desirable. Here, a magnetization study of a single crystal of the $DyFe_5Al_7$ compound is presented.

2. Experimental details

The $DyFe_5Al_7$ single crystal was grown by a modified Czochralski method in a tri-arc furnace from a stoichiometric mixture of the pure elements (99.9% Dy, 99.98% Fe and 99.999% Al). For the crystal structure determination, a standard powder

---

* Corresponding author at: Institute of Physics, Academy of Sciences, Na Slovance 2, 182 21 Prague, Czech Republic.
E-mail address: gorbunov@fzu.cz (D.I. Gorbunov).

0925-8388/$ – see front matter © 2011 Elsevier B.V. All rights reserved.
doi:10.1016/j.jallcom.2011.11.020

X-ray diffraction analysis was performed on a part of the single crystal crushed into a fine powder. The diffraction patterns were refined by means of Rietveld analysis using the Fullprof/Winplotr software [8]. The lattice parameters, $a = 868.9$ pm, $c = 504.2$ pm, are in agreement with the literature [2]. The back-scattered Laue patterns were used to check the monocrystalline state and to orient the crystal to cut the samples for the magnetization measurements.

Temperature and field dependences of the magnetization at 2–280 K were measured along the principal crystallographic directions [1 0 0], [1 1 0] and [0 0 1] of a 30 mg sample using a standard PPMS-14 magnetometer (Quantum Design) in magnetic fields up to 14 T.

3. Results and discussion

Fig. 1 shows magnetization curves (without details of the magnetic hysteresis to be shown and discussed below) measured along the [1 0 0], [1 1 0] and [0 0 1] axes of the $DyFe_5Al_7$ single crystal at several selected temperatures. The compound exhibits spontaneous magnetization along the [1 0 0] and [1 1 0] axes, whereas there is no spontaneous component along the [0 0 1] direction. Therefore, the magnetic moments of $DyFe_5Al_7$ lie in the basal plane of the tetragonal lattice, in agreement with neutron diffraction data [4]. Clear difference between the curves measured along the [1 0 0] and [1 1 0] axes points to a strong anisotropy within the basal plane with the [1 0 0] axis being the easy-magnetization direction. Ratio of the spontaneous moments along the [1 1 0] and [1 0 0] axes ($1.55\mu_B$ and $2.12\mu_B$, respectively, at 2 K) $M_s^{110}/M_s^{100} \approx \cos 45^\circ$ corresponds well to the tetragonal symmetry and reflects good quality of the crystal and its proper orientation.

Temperature dependences of M_s determined from the magnetization isotherms along the [1 0 0] axis and its projection onto the [1 1 0] axis are presented in Fig. 2. The compound has the compensation point at $T_{comp} = 93$ K and $T_C = 231$ K. Both values are in good agreement with those obtained in [2–4] for polycrystalline samples. Assuming that the Dy magnetic moment in the ground state of $DyFe_5Al_7$ is equal to the moment of a free Dy^{3+} ion, $M_{Dy} = 10\mu_B$, and the magnetic structure is collinear and antiparallel, the total moment of the Fe sublattice can then be determined as $M_{Fe} = M_{Dy} - M_s = 7.9\mu_B$, which corresponds to $\mu_{Fe} = 1.6\mu_B$ for an average moment of the Fe atom. Such a high M_{Fe} value practically excludes the possibility of a non-parallel arrangement within the Fe sublattice which can originate from the presence of AF coupling between the Fe atoms in the 8f sites, as it was observed for the isostructural $LuFe_5Al_7$ compound with non-magnetic Lu [9]. Perhaps, negative interactions within the Fe sublattice are suppressed by the Dy–Fe interactions, which lead to the formation of the collinear ferrimagnetic structure. A close μ_{Fe} value ($1.65\mu_B$) was found on a single crystal of $LuFe_6Al_6$ which is evidently a collinear ferromagnet [10].

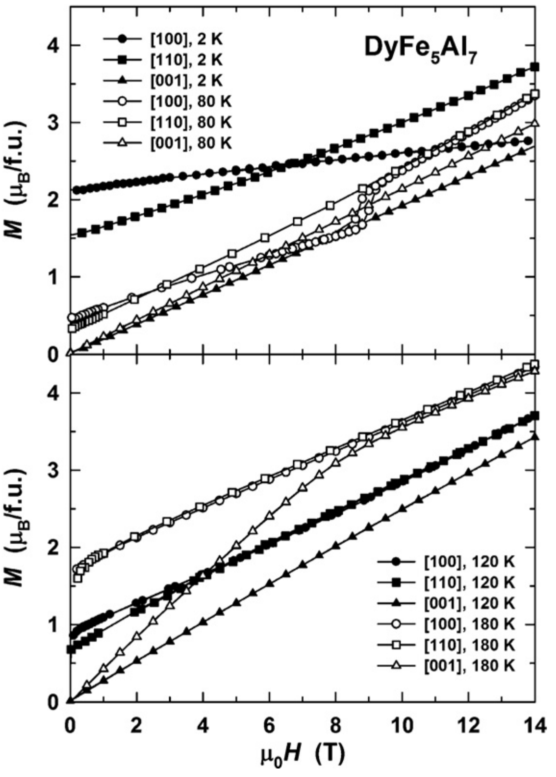

Fig. 1. Magnetization isotherms measured along the principal axes of a $DyFe_5Al_7$ single crystal at selected temperatures.

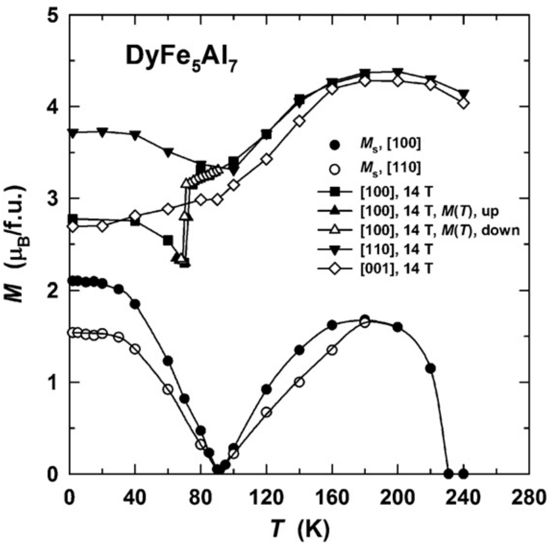

Fig. 2. Temperature dependence of the spontaneous moment M_s obtained from magnetization isotherms along the [1 0 0] axis and its projection onto the [1 1 0] axis and temperature dependence of magnetization measured in 14 T taken from magnetization isotherms along the principal axes. For the [1 0 0] axis, direct $M(T)$ data in 14 T in the vicinity of T_{comp} are included.

A high magnetic susceptibility above the spontaneous magnetization even along the easy magnetization direction can be attributed to a strong bending of magnetic moments with increasing magnetic field. The bending of the moments is more intensive along the [1 1 0] direction. As a result, the magnetization isotherms along the [1 0 0] and [1 1 0] axes intersect at a certain field at temperatures below 100 K. At 80 K, a hysteretic transition is seen in Fig. 1 along the easy [1 0 0] direction in a field ~9 T. Above the transition, the curves along the [1 0 0] and [1 1 0] axes coincide. At 120 K, the transition is no longer seen and the two curves are almost identical except in the low-field region (<4 T). The temperature evolution of the transition will be discussed below. Finally, the in-plane anisotropy vanishes at 180 K (it is also seen in Fig. 2, where M_s^{100} and M_s^{110} coincide) whereas the anisotropy between the basal plane and the c axis persists up to T_C. As seen from Fig. 1, the anisotropy field H_a is still rather high, about 8 T at 180 K.

The magnetization curves along the [1 0 0] axis presented in Fig. 3 show that the transition with the hysteresis of ~0.5 T is seen between 75 and 100 K. The critical field H_{cr} of the transition decreases rapidly upon approaching T_{comp} from above and below. Fig. 4 shows that H_{cr} falls down to 2–3 T at 90 and 95 K. The temperature dependence of H_{cr} shown in Fig. 5 is very sharp. Extrapolation of $H_{cr}(T)$ to low temperatures explains why we did not observe the transition below 70 K: the H_{cr} values exceed the maximum applied field of 14 T. The transition is observed above T_{comp} as well. Above 100 K, it becomes broad and is smeared out at 120 K. The transition is reflected also in the temperature dependence of magnetization in a maximum field of 14 T (Fig. 2). Magnetization along the [1 0 0] axis

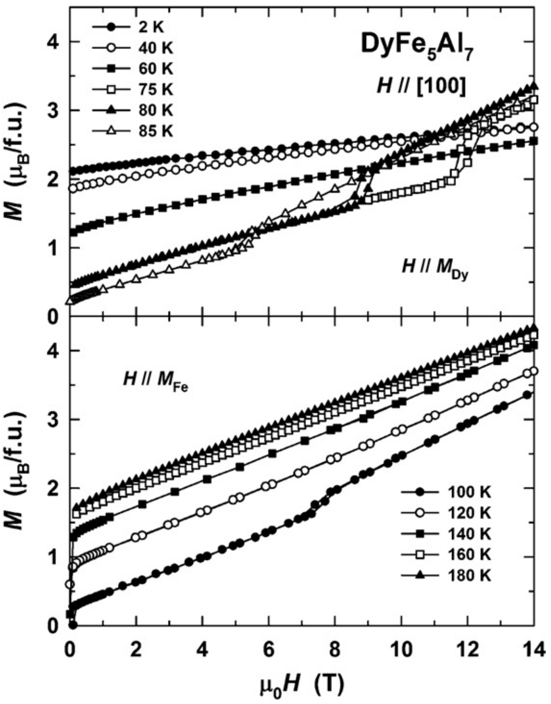

Fig. 3. Temperature evolution of the [1 0 0] axis magnetization curve below (top) and above (bottom) the compensation point $T_{\mathrm{comp}} = 93$ K.

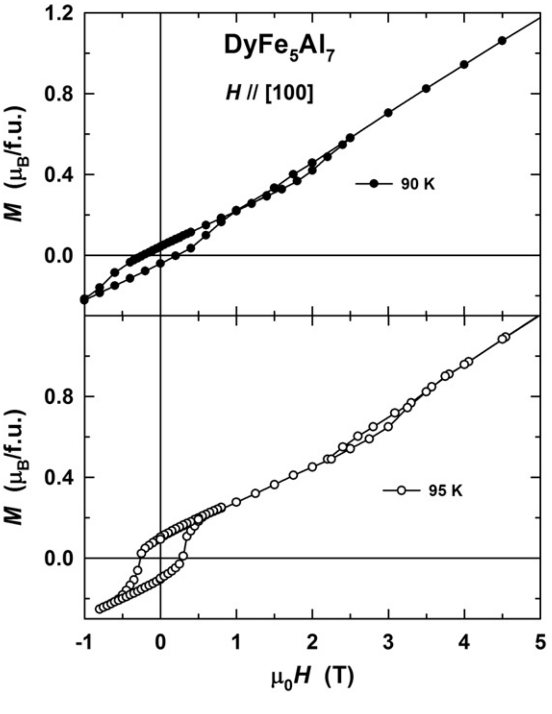

Fig. 4. Magnetization isotherms measured along the [1 0 0] axis in the vicinity of T_{comp}.

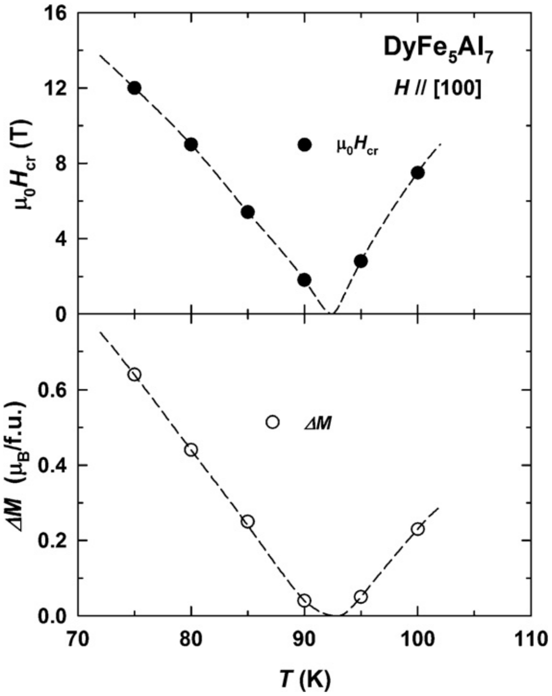

Fig. 5. Temperature dependence of the critical field $\mu_0 H_{\mathrm{cr}}$ of the field-induced transition and of magnetization gain ΔM at the transition.

is considerably lower than along the [1 1 0] axis below 70 K and is expected to reach the latter by the jump at a higher field. At 70–74 K, the step with 2 K hysteresis is observed, and the magnetization is the same along both axes above 80 K.

Since below T_{comp} the magnetic field is parallel to the magnetic moments of the Dy sublattice, the transition can be considered as breaking of the antiparallel coupling between the Dy and Fe sublattices and rotation of the Fe moments. In this case, the Dy sublattice should rotate upon the transition above T_{comp}. However, the interpretation of the transition as occurring in only one of the sublattices contradicts the temperature dependence of the magnetization jump ΔM upon the transition (Fig. 5). First, the observed ΔM is rather small, not exceeding $0.8\mu_B$/f.u. (at 75 K), whereas the magnetic moment of each sublattice should be an order of magnitude higher. Second, $\Delta M(T)$ approaches zero at T_{comp}, i.e., it clearly follows the temperature dependence of the total moment and not those of individual sublattice moments which should be rather flat in such narrow temperature interval and certainly do not pass through zero. The non-monotonous behavior of $H_{\mathrm{cr}}(T)$ passing through zero at T_{comp}, similarly to $\Delta M(T)$, also contradicts the notion of a transition in only one sublattice. Therefore, the transition should involve rotation of both the Dy and Fe sublattices.

In the basal plane of the tetragonal crystal, the [1 0 0] and [0 1 0] crystallographic directions are both the easy magnetization directions. Let us consider two possible orientations of the magnetic moments of Dy and Fe sublattices in a relatively small field applied along the [1 0 0] axis (Fig. 6). In this figure α and φ denote the angles between M_{Fe} and M_{Dy} and between M_{Dy} and the [0 1 0] axis, respectively. It is evident that the anisotropy energy for these two cases is similar, while the Zeeman energy depends on the value of the spontaneous magnetization. For $M_s > 0$ in a small field the Dy and Fe magnetic moments will be oriented along the [1 0 0] direction. However, the susceptibility for a collinear ferrimagnet in this direction is expected to be low. On the other hand, near the compensation point the value of the susceptibility due to the sublattice bending is higher for the case when the magnetic sublattices are oriented normal to the field direction. Therefore, with increasing field we can expect the spin-reorientation transition of M_{Dy} and M_{Fe} from [1 0 0] to a direction close to the [0 1 0] axis. The higher the spontaneous moment, the higher should be the transition field. At very high fields, the ferromagnetic saturation along the field direction will be reached. Hence, in high fields we can expect the inverse transition of the moments from nearly [0 1 0] to the [1 0 0] direction.

In order to estimate the critical fields of the spin-reorientation transitions let us consider the free energy of the system comprising

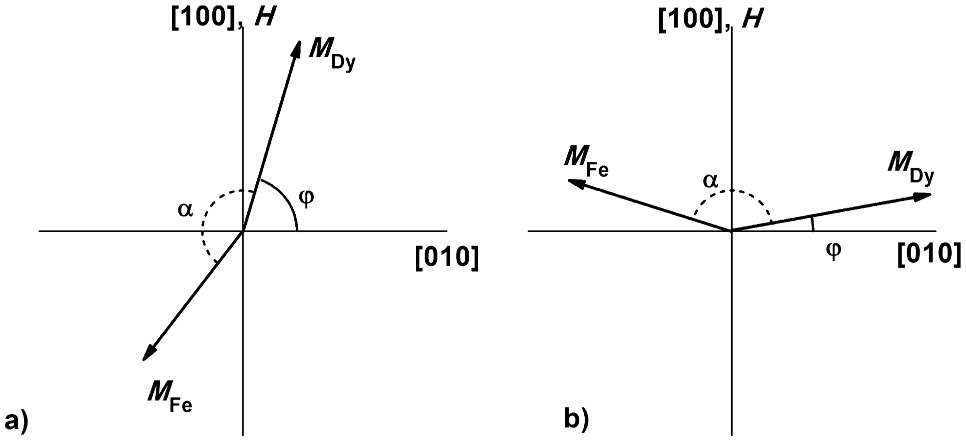

Fig. 6. Possible orientations of the magnetic moments of the Dy and Fe sublattices in a field applied along the [1 0 0] axis: low field (a) and higher field (b).

the energies of intersublattice exchange interaction, magnetic anisotropy and the Zeeman energy:

$$E(\alpha,\varphi,B) = M_{\mathrm{Dy}}\,M_{\mathrm{Fe}}n_{\mathrm{DyFe}}\,\cos(\alpha) - K\,\cos(4\varphi) - \mu_0 H[M_{\mathrm{Dy}}\,\sin(\varphi) + M_{\mathrm{Fe}}\,\sin(\alpha+\varphi)], \qquad (1)$$

where K is the in-plane anisotropy constant, and n_{DyFe} is the intersublattice exchange parameter. Here we neglect the anisotropy of the Fe sublattice. In order to determine the equilibrium angles α_0 and φ_0 of the orientation of the magnetic moments in a magnetic field H we should find the minimum of the free energy (1) with respect to the angles α and φ. Then the magnetization curve will be given by the expression:

$$M(H,\alpha_0,\varphi_0) = M_{\mathrm{Dy}}\,\sin(\varphi_0) + M_{\mathrm{Fe}}\,\sin(\varphi_0+\alpha_0) \qquad (2)$$

The exchange parameter n_{DyFe} for $\mathrm{DyFe_5Al_7}$ can be estimated using the molecular field theory for a collinear two-sublattice ferrimagnet. Comparing the magnetic ordering temperatures of the $\mathrm{RFe_5Al_7}$ compounds with different R elements [2] one can conclude that the energy of the Fe–Fe exchange interaction is much higher than that of the R–R interactions in these compounds. For this case temperature dependence of the magnetic moment of the Dy sublattice is determined by the Dy–Fe exchange interaction:

$$M_{\mathrm{Dy}}(T) = M_{\mathrm{Dy}}(0)B_J\left(\frac{g_J J\mu_{\mathrm{B}}\mu_0 H_{\mathrm{mol}}}{k_{\mathrm{B}}T}\right), \qquad (3)$$

where B_J is the Brillouin function, J the quantum number of the total moment of Dy ion, g_J the Landé factor, and H_{mol} the molecular field at the Dy ion produced by the Fe magnetic moments. The value of the molecular field is proportional to the Fe sublattice magnetic moment, $\mu_0 H_{\mathrm{mol}} = n_{\mathrm{DyFe}}\,M_{\mathrm{Fe}}$, and its temperature dependence is determined by the temperature dependence of the Fe sublattice magnetization:

$$H_{\mathrm{mol}}(T) = \frac{H_{\mathrm{mol}}(0)\,M_{\mathrm{Fe}}(T)}{M_{\mathrm{Fe}}(0)}. \qquad (4)$$

Typically, temperature behavior of the Fe magnetic moment can be taken from the $M(T)$ dependence for an isostructural compound of a similar composition with a non-magnetic R element. However, for $\mathrm{LuFe_5Al_7}$, the magnetization is lowered and its temperature dependence is complicated because of the competition between positive and negative exchange interactions in the Fe sublattice [9]. Therefore, for estimation we used the $M(T)$ dependence for the $\mathrm{LuFe_6Al_6}$ compound with collinear ferromagnetic structure [10]. Reducing this dependence to the values of M_{Fe} and T_{C} for $\mathrm{DyFe_5Al_7}$ and subtracting it from the experimental $M_{\mathrm{s}}(T)$ curve (Fig. 2) we obtained the temperature dependence of M_{Dy} for $\mathrm{DyFe_5Al_7}$. Best fit of the experimental data with Eq. (3) is observed for the molecular field value $\mu_0 H_{\mathrm{mol}}(0) = 42\,\mathrm{T}$, which corresponds to the exchange parameter $n_{\mathrm{DyFe}} = 5.3\,\mathrm{T}/\mu_{\mathrm{B}}$.

Alternatively, the exchange parameter can be estimated from the magnetization curve. In a magnetic field applied along the easy axis at the compensation point the intersublattice exchange parameter is equal to the inverse high-field susceptibility:

$$n_{\mathrm{DyFe}} = \frac{\mathrm{d}(\mu_0 H)}{\mathrm{d}M}. \qquad (5)$$

The experimental magnetization curve at 95 K (Fig. 4) gives $\mathrm{d}(\mu_0 H)/\mathrm{d}M = 4.3\,\mathrm{T}/\mu_{\mathrm{B}}$ that is lower than the value $5.3\,\mathrm{T}/\mu_{\mathrm{B}}$ obtained from $M(T)$ dependence. Therefore, the field-induced bending of magnetic sublattices is somewhat higher than can be expected for the simple collinear two-sublattice model. Nevertheless, in order to calculate the magnetization curves with Eqs. (1) and (2) we fixed the intersublattice exchange parameter to be $n_{\mathrm{DyFe}} = 5.3\,\mathrm{T}/\mu_{\mathrm{B}}$.

For the limiting case $K = 0$, the calculations give the magnetization curve typical of that observed for a free-powder sample [11]. For the field interval $0 < \mu_0 H < n_{\mathrm{DyFe}}(M_{\mathrm{Dy}} - M_{\mathrm{Fe}})$, the ferrimagnetic saturation is realized. At higher fields the canted magnetic structure is formed, and the magnetization linearly increases with field according to Eq. (5). Finally, the ferromagnetic saturation is achieved in the field $\mu_0 H = n_{\mathrm{DyFe}}(M_{\mathrm{Dy}} + M_{\mathrm{Fe}})$.

The anisotropy in the basal plane leads to the formation of two magnetization jumps in the magnetization curve. The values of the critical fields and the shape of the magnetization curve depend on the K value at small K, and are almost independent of K at $K > 10\mu_{\mathrm{B}}\mathrm{T}$. From the magnetization slope along the [1 1 0] direction at different temperatures we can roughly estimate that the in-plane anisotropy constant is $K \sim 50\mu_{\mathrm{B}}\mathrm{T}$ at 0 K and it drops to nearly zero values above 180 K. The calculated T–H magnetic phase diagram is presented in Fig. 7. It is seen that the behavior of the critical field of the transition near the compensation point correlates well with experimental data. At the same time, the values of the calculated and experimental critical fields are different. Better coincidence of the critical fields can be obtained at higher values of intersublattice exchange parameter, but this contradicts the high-field susceptibility data at T_{comp}. Moreover, in fields below H_{crit} the calculations give no bending of sublattice magnetic moments, while the experimental magnetization curve is characterized by a nonzero susceptibility along the easy axis. All these data point to the formation of noncollinear magnetic structure of the Fe moments in magnetic fields. To understand the transition more deeply, it is necessary to observe it at low temperatures and compare the ΔM value with sublattice moments in the ground state. Such experiment requires much higher magnetic fields and is in progress.

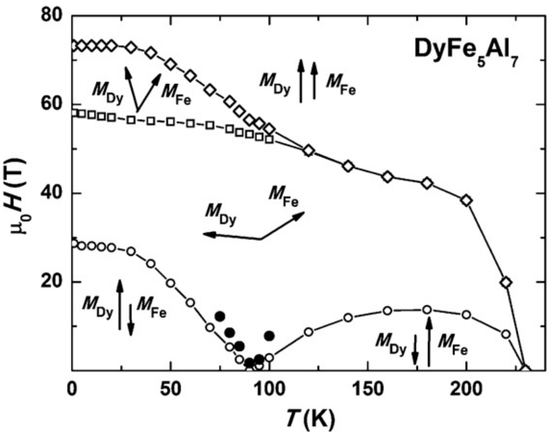

Fig. 7. The calculated T–H magnetic phase diagram. M_{Dy} and M_{Fe} denote the vectors of the Dy and Fe sublattice magnetizations, respectively.

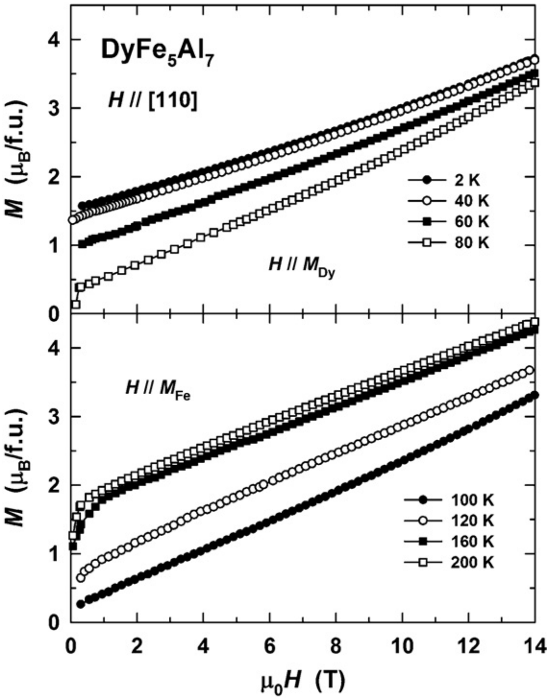

Fig. 8. Temperature evolution of the [1 1 0] axis magnetization curve below (top) and above (bottom) T_{comp}.

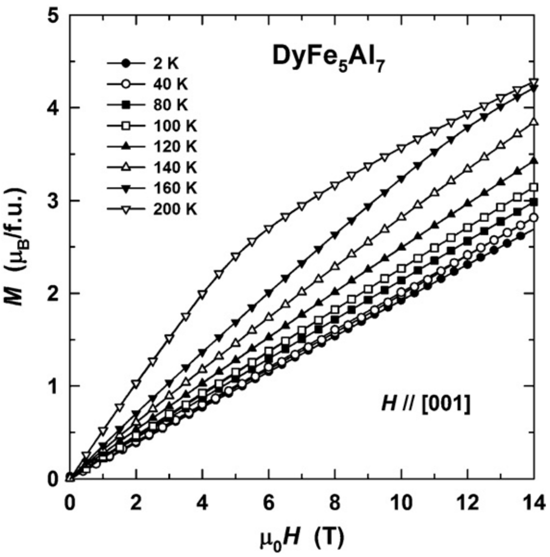

Fig. 9. Temperature evolution of the [0 0 1] axis magnetization curve.

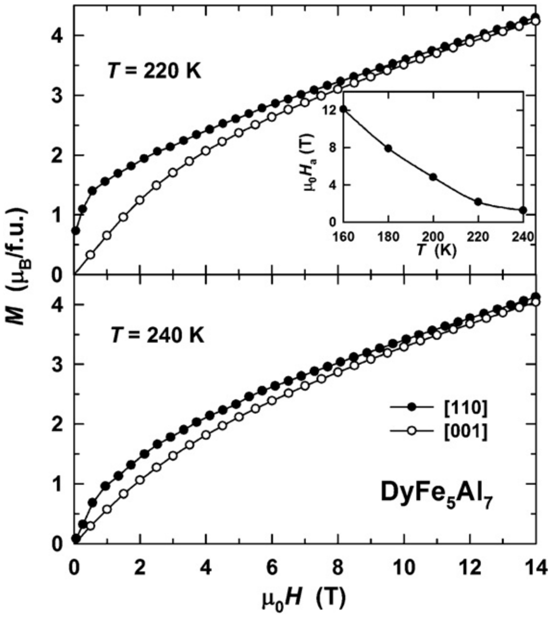

Fig. 10. Magnetization curves along the [0 0 1] and [1 1 0] axes at 220 K and 240 K. The inset shows the temperature dependence of the anisotropy field determined by the SPD method.

Fig. 8 shows magnetization curves along the [1 1 0] axis at different temperatures. Below 120 K, the curves are characterized by small positive curvature. This can be considered a precursor to a transition at higher fields. At higher temperatures, the magnetization isotherms become practically linear up to T_C. The $M(H)$ curves measured along the [0 0 1] axis (Fig. 9) are linear below 160 K, which shows that the anisotropy field H_a exceeds maximum field 14 T applied in the experiment. This is also clearly seen from Fig. 2 where $M(T)$ in 14 T measured along [0 0 1] is lower than that in the basal plane (in particular, along the [1 1 0] axis). A change of the $M(H)$ curve's slope reflecting H_a appears only at 160 K at about 12 T and at lower fields at higher temperatures. Magnetization curves just below and just above T_C along the basal plane and the [0 0 1] axis are presented in Fig. 10. It is seen that the magnetic anisotropy persists even in the paramagnetic state. The inset in Fig. 10 shows temperature dependence of H_a in the temperature range where the H_a values do not exceed the maximum applied field 14 T. H_a was determined by the SPD (singular-point detection) method [12] as the field corresponding to the minimum of d^2M/dH^2 for the hard-axis magnetization curve.

For clarity we presented in Figs. 1, 3 and 8 only the field-descending branch of the magnetization curves in the basal plane or, in the case of the transition, also ascending part but only above 4 T. Now we will describe a domain hysteresis observed in the DyFe$_5$Al$_7$ single crystal. Figs. 11 and 12 show hysteresis loops in a field applied along the [1 0 0] and [1 1 0] axes, respectively, at different temperatures. The coercive field H_c is very large especially taking into account the easy-plane type of magnetic anisotropy. H_c reflects the fact that, apart from the anisotropy between the basal plane and the tetragonal axis, the in-plane anisotropy is also very strong in DyFe$_5$Al$_7$. At 2 K, H_c reaches very large values of 3 T and 2.4 T along the [1 0 0] and [1 1 0] axes, respectively, and rapidly decreases with increasing temperature (Fig. 13). Below approx. 20 K, $H_c(T)$ exhibits a drastic exponential

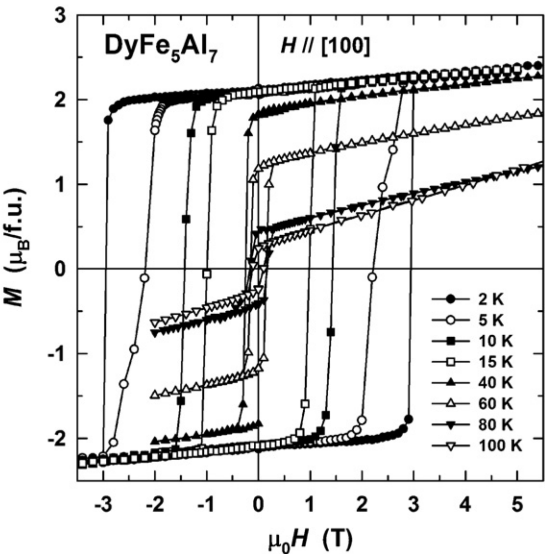

Fig. 11. Low-field details of hysteresis loops measured along the [1 0 0] axis at different temperatures.

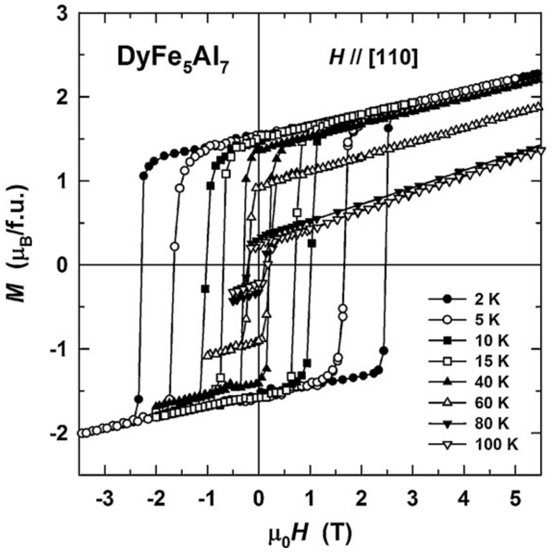

Fig. 12. Low-field details of hysteresis loops measured along the [1 1 0] axis at different temperatures.

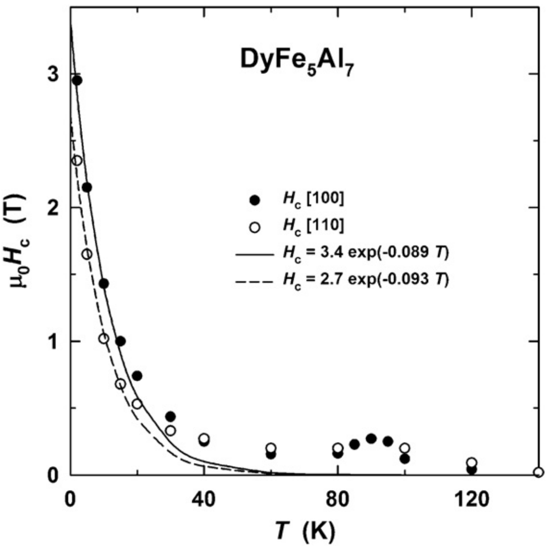

Fig. 13. Temperature dependence of the coercive field $\mu_0 H_c$ along the [1 0 0] and [1 1 0] axes. The dashed lines represent the fit $\mu_0 H_c = \mu_0 H_c(0)\exp(-\beta T)$.

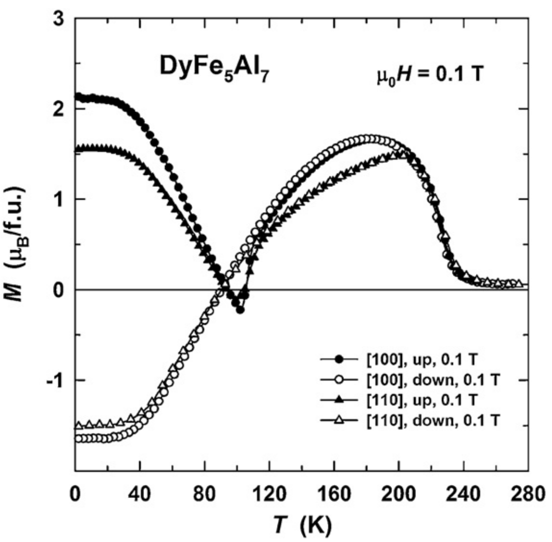

Fig. 14. Temperature dependence of magnetization measured in a 0.1 T field applied along the [1 0 0] and [1 1 0] axes. First the sample was cooled to 2 K in a 0.5 T field. Then, the magnetization was measured in 0.1 T upon heating the sample up to 280 K and subsequent cooling down to 2 K.

decrease $H_c(T) = H_c(0)\exp(-\beta T)$ corresponding with the model of high intrinsic coercivity of narrow domain walls applicable to systems with very high magnetic anisotropy [13]. At higher temperatures, a different less temperature-dependent mechanism of coercivity dominates leading to a much slower decrease in H_c with a moderate maximum in the vicinity of T_{comp}.

Apart from the field hysteresis, $DyFe_5Al_7$ also exhibits thermal hysteresis. Fig. 14 shows the temperature dependence of magnetization measured in a 0.1 T field applied along the main axes in the basal plane upon heating and cooling. First, the sample was cooled down from room temperature to 2 K in a magnetic field of 0.5 T. Since this field is considerably higher than the coercivity just below T_{comp}, the crystal became saturated along the moments of the Dy sublattice. Qualitatively the same result was obtained in refs. [2,3] under the same conditions. Upon heating this single-domain sample in a field of 0.1 T through the compensation point, the magnetization does not reorient itself along the moments of the Fe sublattice, i.e., it becomes negative with respect to the applied field of 0.1 T because the coercivity is larger than this field in the vicinity of T_{comp} (Fig. 13). However, the magnetization remains negative only in a narrow temperature interval because above 100 K H_c becomes lower than the applied field and the crystal becomes magnetized along the field. Upon subsequent cooling the sample, since H_c below T_{comp} is always higher than 0.1 T, the crystal remains single-domain after the inversion of magnetization from the Fe to the Dy sublattice, and the "negative magnetization effect" is seen in a wide range up to the lowest temperatures. Under particular conditions of the experiment, "the single-domain state" is valid, however, only for the [1 1 0] axis where magnetization of the cooled crystal reaches at 2 K the absolute value of $1.55\mu_B$, i.e., the same as the projection of M_s onto this axis. For the [1 0 0] axis, a slightly lower minimal H_c below T_{comp}, (at 60–80 K), 0.16 T instead of 0.2 T along [1 1 0], leads to a partially demagnetized state, and the absolute value of the negative magnetization at 2 K ($1.7\mu_B$) is lower than $M_s = 2.1\mu_B$.

4. Conclusion

Magnetic studies of a $DyFe_5Al_7$ single crystal with the tetragonal $ThMn_{12}$-type structure have been presented for the first time. $DyFe_5Al_7$ orders ferrimagnetically at $T_C = 231$ K and exhibits a compensation of the Dy and Fe sublattice magnetic moments at $T_{comp} = 93$ K. Magnetization isotherms measured along the principal crystallographic directions indicate that the magnetic moments lie in the basal plane of the tetragonal lattice. The anisotropy between the basal plane and the [0 0 1] axis is rather high, the anisotropy field considerably exceeds the maximum applied field of 14 T at low temperatures. Moreover, a strong anisotropy within the basal plane is also seen, with the [1 0 0] axis being the easy magnetization direction with the spontaneous magnetic moment of $2.1\mu_B$. After reaching a single-domain state, the magnetic isotherms along the [1 0 0] and [1 1 0] directions do not saturate, which is a consequence of a strong bending of magnetic moments with increasing magnetic field. A very high coercivity with H_c values up to 3 T was found at 2 K. With increasing temperature, the coercivity decreases rapidly, passes through a weak maximum at T_{comp} and becomes negligible at $T > 120$ K.

In the temperature range 75–100 K, the compound displays a field-induced magnetic transition along the easy [1 0 0] direction. Temperature dependence of the critical field H_{cr} of the transition is very strong, H_{cr} evidently exceeds 14 T below 75 K. We developed a simple model of the spin-reorientation transition within the basal plane, which allows us to explain qualitatively the observed temperature behavior of H_{cr} near the compensation point. It is desirable to study magnetic isotherms along the principal crystallographic directions at much higher magnetic fields.

Acknowledgements

The work is a part of the research project AVOZ10100520 of Academy of Sciences of Czech Republic and has been supported by Czech Science Foundation (grant 202/09/0339).

References

[1] W. Suski, in: K.A. Gschneidner Jr., L. Eyring (Eds.), Handbook on the Physics and Chemistry of Rare Earths, vol. 22, North-Holland, Amsterdam, 1996, p. 143.
[2] I. Felner, I. Nowik, M. Seh, J. Magn. Magn. Mater. 38 (1983) 172.
[3] I. Felner, I. Nowik, K. Baberschke, G.J. Nieuwenhuys, Solid State Commun. 44 (1982) 691.
[4] W. Kockelmann, W. Schäfer, G. Will, P. Fischer, J. Gal, J. Alloys Compd. 207–208 (1994) 311.
[5] W. Shäfer, W. Kockelmann, G. Will, P. Fischer, J. Gal, J. Alloys Compd. 225 (1995) 440.
[6] O. Moze, R.M. Ibberson, K.H.J. Buschow, J. Phys.: Condens. Matter 2 (1990) 1677.
[7] N.P. Duong, E. Brück, F.R. de Boer, K.H.J. Buschow, J. Alloys Compd. 338 (2002) 213.
[8] http://www.ill.eu/sites/fullprof/.
[9] D.I. Gorbunov, A.V. Andreev, N.V. Mushnikov, submitted for publication.
[10] A.V. Andreev, Physica B 321 (2009) 2978.
[11] J.P. Liu, F.R. de Boer, P.F. de Châtel, R. Coehoorn, K.H.J. Buschow, J. Magn. Magn. Mater. 132 (1994) 159.
[12] G. Asti, S. Rinaldi, J. Appl. Phys. 45 (1974) 3600.
[13] H.R. Hilzinger, H. Kronmüller, Phys. Status Solidi B 54 (1972) 593.